IEEE Access
Multidisciplinary | Rapid Review | Open Access Journal

Received March 25, 2020, accepted May 2, 2020, date of publication May 8, 2020, date of current version May 21, 2020.

Digital Object Identifier 10.1109/ACCESS.2020.2993288

Theoretical and Experimental Evaluation of a Thermoelectric Generator Using Concentration and Thermal Energy Storage

XIAOMEI SUI[1,2], WENBIN LI[1], YUQI ZHANG[1], AND YAFENG WU[1]

[1]Key Lab of State Forestry and Grassland Administration for Forestry Equipment and Automation, School of Technology, Beijing Forestry University, Beijing 10083, China

[2]School of Electronic and Information Engineering, North China Institute of Science and Technology, Langfang 065201, China

Corresponding author: Wenbin Li (leewb@bjfu.edu.cn)

This work was supported in part by the National Natural Science Foundation under Grant 31670716 and in part by the Key Lab of State Forestry and Grassland Administration for Forestry Equipment and Automation.

ABSTRACT To improve the thermoelectric conversion efficiency of solar thermoelectric power, a concentration solar thermoelectric generator (CTEG) unit based on concentrating and storing energy is designed. A Fresnel lens is used to concentrate thermal energy, and a phase change material (PCM) is used to store thermal energy to increase the temperature difference between the hot and cold ends of thermoelectric (TE) sheets. The heat stored in the PCM container will help to generate continuous solar energy at night and improve the thermal power conversion efficiency of the TEGs. The energy conversion equilibrium equation is established for the CTEG unit. By numerical calculation, we conclude that the absorption rate of the coating surface is reduced by 0.1 and the maximum thermoelectric conversion efficiency is reduced by approximately 0.4%. By selecting different heights of the heat exchanger, the unit supplies 1.025 v, 0.4204 v and 0.299 v open circuit voltages on average for approximately 30, 44 and 53 minutes, respectively. Therefore, the height of the heat exchanger affects the rate of heat energy absorption and release. The reversible operation of the CTEG-PCM unit is conducive to the day and night operation of solar power generation and is more suitable to solving the self-supplying power problem for wireless temperature sensors in forests.

INDEX TERMS Energy storage, phase change material, solar power generation, thermoelectric generator.

I. INTRODUCTION

The main bottleneck of wireless sensor network (WSN) applications is the power supply of each node. WSN nodes are low-power consumption electronic devices, and chemical batteries are the main mode of supply; however, in this mode, the battery needs to be replaced regularly to ensure that the WSNs can continue to work [1]–[3]. Because of the inconvenience and high cost caused by the replacement of batteries in forest areas, the shortcomings of chemical batteries have been gradually emerging. Therefore, how to collect all kinds of energy in the environment to supply power for WSN nodes has been increasing [4], [5]. The key issue for WSN nodes is the long-term stability of the power supply, not the short-term solution. Energy collected from the environment is stored to obtain the energy for sensing and communication.

A thermoelectric generator (TEG) is a kind of solid-state device that can generate electricity directly from a heat source. The working principle of the TEG is to convert the temperature difference into electric energy based on the Seebeck effect. Compared with traditional systems, the development and application of TEGs have limiting factors such as low conversion efficiency and high capital costs. However, the advantage of TEG's lies in using low-level thermal energy without high costs and solar thermal energy, and its commercial availability is not restricted by its low efficiency. The available TEG efficiency is very low, and as a feasible tool for power generation, a significant improvement in the conversion efficiency is needed [6], [7].

Solar energy is easy to use, but the energy density of solar radiation reaching the Earth's surface is very low and constantly changing. To maintain the stable and uninterrupted operation of the heating or power supply, it is necessary to store solar energy and release it when the solar energy is insufficient. The stored energy can meet the needs of

The associate editor coordinating the review of this manuscript and approving it for publication was Xiaodong Liang.

a continuous and stable energy supply for production and living. As an effective way to solve the contradiction between the energy supply time and space, a phase change heat storage system is an important technology for improving energy utilization.

The application of phase change material (PCM) for thermal energy storage has affected the development of TEGs and has been helpful for extending the duration of heating or cooling during the process of power generation [8], [9]. Agbossou *et al.* [10] designed a work unit made of PCM and a TEG. These researchers used a numerical simulation method to test the system performance. During the process of the numerical calculation, special attention was paid to the realization of the environmental load, including solar radiation, temperature change and wind speed. The calculation results show that the work unit can collect micro energy day and night by virtue of the heat storage of the PCM. Zhang *et al.* [11] further applied the above research to experimental investigations. These investigators used hydrated salt with a melting point of approximately 28°C. To facilitate night power generation, the hot side of the TEG is exposed to air cooling. Jaworski *et al.* [12] used capric acid with a melting point of approximately 30.5°C as the PCM. They studied the effect of thermoelectric power generation under PCM refrigeration and measured the open circuit voltage and the loop current of the circuit. Furthermore, these authors evaluated the performance characteristics of the TEG. Their results confirmed the potential of the application of PCM as a cooling/heating media in TEGs. Tu *et al.* [13] developed and experimentally analysed the application of PCM in thermoelectric power generation devices with considerable temperature changes from 100°C to - 50°C. The PCM used was a paraffin-based composite material. Atouei *et al.* [14] proposed a prototype of a new two-stage TEG system integrated with the PCM. These researchers used the PCM box as the first TEG level radiator and the second TEG level heat source. In the second stage, five smaller TEG modules are installed around the PCM with an independent heat sink, which can be naturally cooled. The proposed design makes the TEG system more suitable for WSN applications. The experimental results show that the proposed two-stage TEG system generates an average of 27% more potential than the first-stage TEG system. Furthermore, to conduct a comprehensive experimental investigation, Atouei *et al.* [15] manufactured two aluminium boxes with different structures filled with PCM. These aluminium boxes were applied to the hot side, cold side and both sides of the TEG module in three configurations. These researchers compared the effect of the PCM aluminium box used in different positions with an ordinary TEG system without a PCM. The results show that the PCM can not only generate voltage for a longer time after removing the external heat source but also protect the TEG module from high thermal power. Krishnadass. [16] focused on the application of D-mannitol for the integration of the PCM and TEG module. The system realized the reversible operation of heating and cooling of the TEG module by storing heat energy in the PCM. The experimental evaluation of heating and cooling of the TEG module was carried out. The results show that the reversible operation of the TEG module is conducive to the day and night cycle operation of solar power generation. Kiziroglou *et al.* [17] proposed a thermal storage device for a thermal engine structure monitoring system. The device uses a PCM-filled thermal storage unit to generate the internal space temperature difference when the ambient temperature changes frequently. At the same time, the key design parameters and characterization methods of these devices are defined, and the expected maximum electric energy density is calculated in a given temperature range. The proposed device provides a unique power supply solution for WSN applications involving temperature changes. Zhao [18] introduced a prototype thermoelectric system with the integration of space cooling and PCM heat storage, and evaluated the effectiveness of PCM heat storage through an experimental comparison between different working modes. The experimental results showed that the power conversion rate of the system can be increased by 35.3% by using PCM.

In combination with the utilization of solar collectors, some scholars have carried out experimental research [19], [20]. Atik [21] studied the thermoelectric performance of a solar receiver. The results show that the collector surface temperature and power efficiency are determined by different radiation intensities and concentration ratios. In the new photovoltaic thermoelectric power generation system designed by Cui [22], PCMs are used to reduce the temperature fluctuation of the photovoltaic (PV) cells and thermoelectric (TE) modules and to keep the hybrid PV-TE system running under fixed operating conditions. These authors obtained relatively good results. Hasan [23] conducted an experimental investigation on electric heating and cogeneration systems through a thermoelectric module. In the design, a Fresnel lens and thermoelectric module are used to gather the solar beam and generate electric energy.

Although solar energy heat is often affected by changes in atmospheric conditions, it can be used to drive microdevices or thermoelectric circuits and operate as a small independent power supply [24]. A review of the literature shows that PCMs and TEGs are good candidates as hybrid storage-harvesting energy systems. However, few studies have aimed to link concentration, thermoelectric effects and PCM effects in a thermoelectric system. In this study, a small power generation prototype which is composed of a concentration solar thermal electric generator (CTEG) and PCM is investigated experimentally. This prototype works under the condition of a Fresnel lens concentrating at the hot end and phase change storage at the cold end. The system was tested for three different exchanger heights to evaluate the application of a PCM for enhancing the available electrical potential for a longer time and to show its suitability for wireless sensor applications.

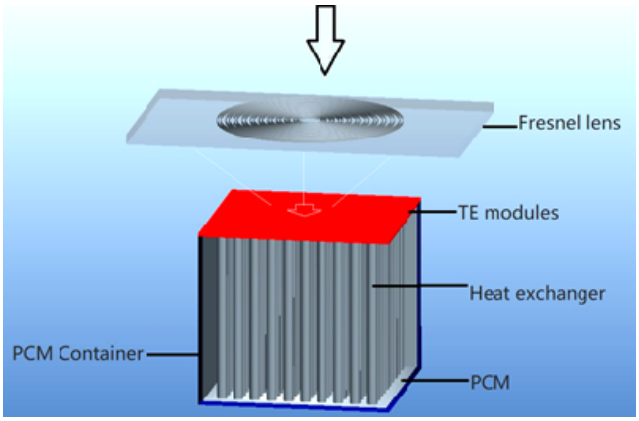

FIGURE 1. Structure of the CTEG-PCM.

II. STRUCTURE OF THE CTEG-PCM

The structure of the CTEG-PCM integrated with a Fresnel lens, TE modules, a heat exchanger and PCM container is shown in Fig. 1.

The incident sunlight is concentrated by Fresnel lenses and then focused onto TE modules. To absorb sunlight more efficiently, a copper sheet coated with a selective absorber is soldered to the surface of the TE modules. The heat exchanger is attached to the other end of the TE module to dissipate heat rejected from the cold end of the TE modules, which keeps them at a low temperature. When the concentrated light covers the absorber surfaces, the concentration ratio can be defined as the ratio of the area of the lens to that of the absorbers. Because thermal energy in the daytime is stored in the PCM container and released at night, TE power generation continues. Compared with regular systems, this design has improved system integration and persistence, decreased system energy losses, and thus increased the total conversion efficiency.

III. MATHEMATICAL MODEL OF THE CTEG

A. CONVERSION EFFICIENCY OF THE CTEG

Based on energy balance analysis, the conversion efficiency of the CTEG-PCM unit can be written as

$$\eta_e = \frac{P_{out}}{Q} = \frac{(Q_{in} - Q_{emi} - Q_{cov})}{Q}\eta_{TE} \tag{1}$$

where P_{out} is the power output of a TE sheet; Q, Q_{in}, Q_{emi}, and Q_{cov} are the sum of the incident sunlight energy on the Fresnel lens, the heat absorbed by the collector, the energy radiated from the collector surface, and the heat energy by natural convection, respectively; and η_{TE} is the conversion efficiency of the TE.

When the solar irradiance is q_{rad} and the area of the Fresnel lens is A_f, the energy incident on the surface of the Fresnel lens is

$$Q = q_{rad}A_f \tag{2}$$

When the sunlight is concentrated by a ratio of C_g, the optical efficiency of the Fresnel lens is η_{opt}, the absorption rate of the selective absorber is α_c, and the surface area of the selective absorber is A_c; therefore, the heat absorbed by the collector can be expressed as

$$Q_{in} = q_{rad} \times C_g \times A_c \times \eta_{opt} \times \alpha_c, \tag{3}$$

where A_c is assumed to be equivalent to the cross-sectional area of the TE and C_g is the concentration ratio, which is the area of the lens divided by that of the selective absorber; i.e., $C_g = A_f/A_c$. The energy radiated from the collector surface, denoted as Q_{emi}, can be calculated as

$$Q_{emi} = \varepsilon\sigma_{BC}A_c(T_1^4 - T_{air}^4) \tag{4}$$

where T_1 is the temperature of the collector surface, T_{air} is the ambient temperature, ε is the emissivity of the collector coating, σ_{BC} is the Stefan-Boltzmann constant, and $\sigma_{BC} = 5.67 \times 10^{-8}(W \cdot m^{-2} \cdot K^{-4})$. The heat energy by natural convection Q_{cov} can be calculated as

$$Q_{cov} = h_{air}A_c(T_1 - T_{air}), \tag{5}$$

where h_{air} is the thermal convection coefficient, $h_{air} = 5.7 + 3.8v$, and v is the speed of the ambient wind [25]. Substituting equations (2)-(5) into equation (1), the thermal efficiency of the CTEG-PCM unit can be obtained as follows:

$$\eta_e = (\eta_{opt}\alpha_c - \frac{\varepsilon\sigma_{BC}}{Q_{rad}C_g}(T_1^4 - T_{air}^4) - \frac{h_{air}}{Q_{rad}C_g}(T_1 - T_{air}))\eta_{TE} \tag{6}$$

It can be seen from (6) that the conversion efficiency of the CTEG-PCM unit depends on the optical efficiency of the lens, the absorption rate of the selective absorber, the concentration ratio and other parameters as well as the conversion efficiency of the TE module.

B. CONVERSION EFFICIENCY OF THE TE MODULE

The complex working conditions of TE devices include a variety of thermoelectric effects, heat conduction, heat convection and heat radiation [26], [27]. At the same time, TE materials have temperature characteristics, such as the Seebeck coefficient, resistivity and thermal conductivity, which are all functions of temperature [28], [29]. To simplify the TE power generation model, it is assumed that the temperature distribution at both ends of the TE module is uniform, the working condition of the TE module is stable, and the cross-sectional area and length of each thermocouple arm are equal, regardless of the Thomson effect. Based on the above assumption, the heat flow into and out of the thermoelectric module Q_h and Q_c can be, respectively, expressed as

$$Q_h = N[\alpha IT_1 + K(T_1 - T_2) - \frac{1}{2}I^2R_{TE}] \tag{7}$$

$$Q_c = N[\alpha IT_2 + K(T_1 - T_2) + \frac{1}{2}I^2R_{TE}] \tag{8}$$

where T_2 is the temperature of the TE cold end, N is the number of thermocouple arms, and α, k, and R_{TE} are the Seebeck

coefficient, the thermal conductance, and the internal resistance of the TE module, respectively. These parameters are calculated as follows:

$$\alpha = \alpha_p + \alpha_n \tag{9}$$

$$k = k_n \frac{S_n}{l_n} + k_p \frac{S_p}{l_p} \tag{10}$$

$$R_{TE} = \rho_n \frac{l_n}{S_n} + \rho_p \frac{l_p}{S_p} \tag{11}$$

where S, l and ρ are the cross-sectional area, the length, and the resistivity of thermocouple arms, respectively. Superscripts n and p indicate the n- and p-types, respectively. In equations (7) and (8), the current I can be calculated as

$$I = \frac{\alpha(T_1 - T_2)}{R_{TE} + R_L} \tag{12}$$

By writing the load resistance in terms of the internal resistance as $R_L = mR_{TE}$ ($m$is the proportional coefficient), the output power by the TE is

$$P_{out} = \frac{m}{(1+m)^2} \times \frac{\alpha^2(T_1 - T_2)^2}{R_{TE}} \tag{13}$$

According to circuit theory, the maximum output power is produced when the load resistance is equal to the total internal resistance; that is, $m = 1$ and $R_L = R_{TE}$. Therefore, the maximum output power P_{max} and the conversion efficiency of the TE module η_{TE} are calculated by using equations (14) and (15).

$$P_{max} = \frac{\alpha^2(T_1 - T_2)^2}{4R_{TE}} \tag{14}$$

$$\eta_{TE} = \frac{P_{out}}{Q_h} \tag{15}$$

Substituting (7), (13) and (15) into (6), the thermal efficiency of the CTEG-PCM unit can finally be obtained.

IV. EXPERIMENTAL

As shown in Fig. 2, the experimental device consists of a Fresnel lens, a TEG, a PCM container and a heat exchanger. The solar radiation shines on the Fresnel lens, and the spot at the focal plane is a circle with a diameter of 10-12 mm, which converges on the copper sheet on the TE module (model: TEC1-12706T200, manufacturer: MELCOR Company). The specifications of the chosen TEM are shown in Table 1. Performance parameters of the TE material are the same as those in reference [30]. The high thermal conductivity of the copper (377 $W{\cdot}m^{-1}{\cdot}K^{-1}$) makes the upper temperature of the TEG uniform. After simple grinding treatment with coarse sandpaper, the upper copper sheet with dimensions of 40×40 × 0.5 mm is coated with a solar selective absorber (model: RLHY-2337, manufacturer: Beijing Rongli Hengye Technology Co., Ltd.,China) on one side. The highest absorption rate of the selective absorber can reach 0.94. The other side of the copper sheet is pasted on the hot end of the TEG by conductive silica gel (Thermal conductivity is greater than 1.5 $W{\cdot}m^{-1}{\cdot}K^{-1}$). The lower copper sheet was simultaneously an upper cover of the PCM container.

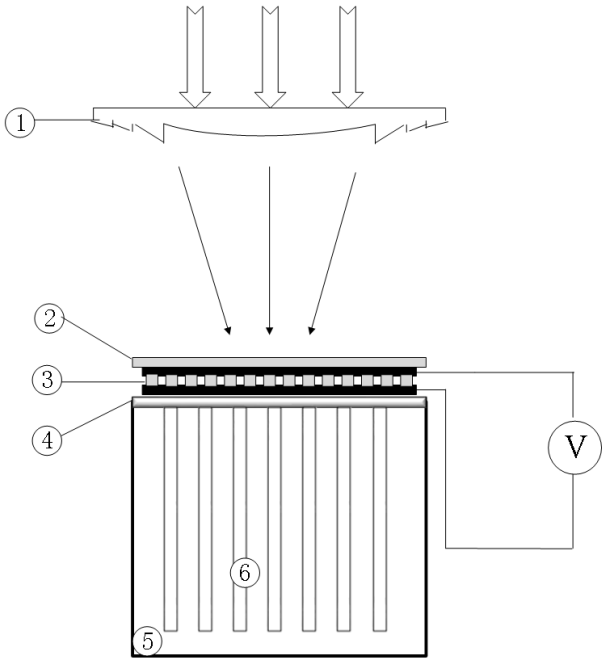

FIGURE 2. Schematic diagram of the experimental device 1-Lens, 2-Upper copper, 3-TEG, 4-Lower copper, 5-PCM container, 6-Heat sink, V-Voltmeter.

TABLE 1. Specifications of the TEC1-12706T200 TE module.

Parameter	Value
Thermoelectric Material	Bismuth Telluride Semiconductor Material
P-N Junctions (couples)	127
Length×Width×Thickness (mm)	40 × 40 × 3.9
P_{max} (W)	56
I_{max} (A)	6
V_{max} (V)	15.4
Internal Resistance (Ω)	2.3
Maximum Operating Temperature (°C)	200

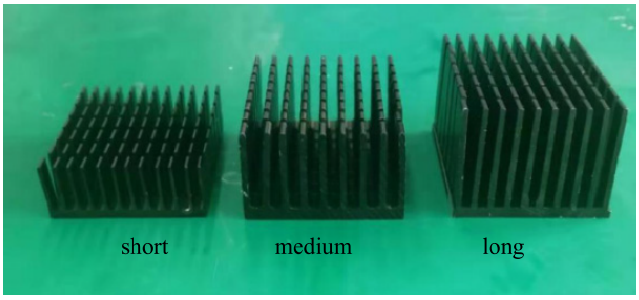

FIGURE 3. Heat exchangers.

The heat exchanger is made of high-quality aluminium, as shown in Fig. 3, which is connected with the cold end of the TEG through the lower copper sheet and placed in the

PCM container. The thickness of the fins is 1.5 mm, the distance between the fins is 3 mm, the fin slotted distance is 3 mm, and the fin heights are 14 mm, 24 mm, and 30 mm, respectively.

Two kinds of paraffin (Shanghai Yijiu Chemical Co., Ltd., China) were used with melting points of 56 °C and 35 °C and latent heats of 255.22 kJ·kg^{-1} and 246.62 kJ·kg^{-1}, respectively. Choosing paraffin was dictated by the fact that these materials are stable, easily available and do not exhibit supercooling, in contrast to the inorganic materials. This material is an ideal low-temperature phase change thermal storage material [31]. Approximately 60 ml of liquid paraffin was poured into the PCM container.

The PCM container is made of heat insulation board (Feintool, model F-800) and has a cubic shape with dimensions of 40 × 40 × 40 mm. The bottom and side walls of the container were insulated by 2 cm thick thermal insulation cotton.

The model of the TEG was equipped with four corrected K-type thermal-couples. The temperatures at the following locations were measured: internal surfaces of copper sheets (i.e., the contact temperatures between copper sheets and thermoelectric modules, T_1, T_2), the PCM temperature at the bottom of the PCM container (T_3) and the temperature of the ambient environment (T_{air}). An automatic digital recorder (measurement accuracy: ±0.2%, MIK-R4000D, Hangzhou Meikong Automation Co., Ltd., China) was used to record the temperatures and the open circuit voltages (U) of the CTEG-PCM. The instantaneous values were recorded every five seconds to ensure the accuracy of the experiment. The solar irradiation intensity was measured every hour by a solar power meter (measurement accuracy: ±10 W/m^2, TES-1333R, TES Electrical Electronic Corp.).

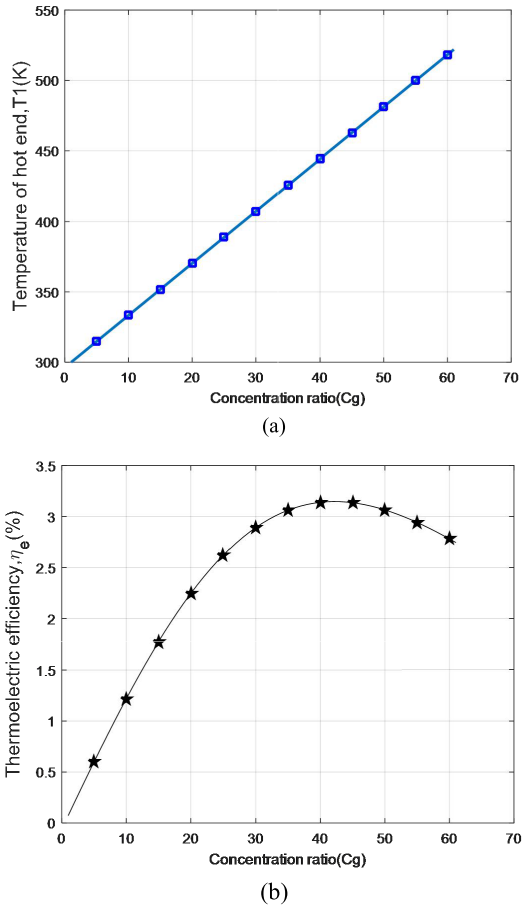

FIGURE 4. Effect of the concentration ratio: (a) on the hot end temperature and (b) on the conversion efficiency.

V. RESULTS AND DISCUSSION

A. EFFECT OF THE CONCENTRATION RATIO ON THE CTEG-PCM

When the area of the heat collector is kept constant, different concentration ratios can be obtained by varying the area of the Fresnel lens. Fig. 4 shows the influence of the concentration ratio on the hot end temperature and conversion efficiency of the CTEG-PCM, and some parameters are shown in Table 2.

Fig. 4a shows that the hot end temperature T_1 of the TEG increases linearly with increasing concentration ratios. Since any thermoelectric material has its own maximum working temperature range, when T_1 reaches the working temperature limit of 525 K of Bi_2Te_3, it can be defined as the limit of the concentration ratio, expressed in C_{gmax}. From Fig. 4b, $C_{gmax} = 60$, beyond which the system will not operate. It can be seen from Fig. 4b that the conversion efficiency also increases with an increase in the concentration ratio first. When the concentration ratio is further increased, the conversion efficiency increases slowly. At C_{gmax}, the conversion efficiency is not the largest, which is caused by the decreased thermoelectric performance of Bi_2Te_3 under high-temperature conditions.

To improve the efficiency of heat absorption in the daytime, copper is placed on the surface of the TEG and coated with a solar selective coating. This method has been tested in the application of solar heat collection and is a successful collection method [32]. At night, the copper above the TEG acts as the equivalent radiator when the PCM is exothermic [33]. The relationship between the conversion efficiency of the CETG unit and the absorption rate of the coating selective absorber is shown in Fig. 5.

Fig. 5 shows that when the concentration ratio is small, the influence of the absorption rate of the coating selective absorber on the conversion efficiency of the system is not obvious. However, the influence of the intensity on the conversion efficiency increases with increasing concentration ratios; specifically, the absorption rate of the coating selective absorber decreases by 0.1, and the conversion efficiency decreases by 0.4% when the conversion efficiency reaches a maximum. In practical applications, when the concentration ratio is small, the absorption rate of the coating selective absorber has little influence on the conversion efficiency of the CTEG unit. At this time, the conversion efficiency of

TABLE 2. Performance parameters used in the numerical simulation.

Parameter	Number Value
Solar irradiance ($W \cdot m^{-2}$)	q_{rad} =900
Optical efficiency of the lens	η_{opt} =0.92
Absorption rate of the selective absorber	α_c =0.9
Emissivity of the collector coating	ε =0.05
Thermal convection coefficient of air ($W \cdot K^{-1} \cdot m^{-2}$)	h_{air} =5.7
Stefan-Boltzmann constant ($W \cdot K^{-4} \cdot m^{-2}$)	$\sigma_{BC}=5.67\times10^{-8}$
Cross-sectional area of the thermocouple arm (m^2)	S =1 x 10^{-6}
Length of the thermocouple arm (m)	l =3.9 x 10^{-3}
Area of the selective absorber (m^2)	A_c =0.0016
Number of thermocouple arms	N=127
Temperature of the cold end (K)	T_2=298
The ambient temperature (K)	Tair=298
Seebeck coefficient of TE materials ($V \cdot K^{-1}$)	$\alpha_n=-\alpha_p$ =(22224.0 + 930.6T − 0.990 5T^2)×10^{-9}
Resistivity of the TE material ($\Omega \cdot m$)	$\rho_n=\rho_p$ =(5112.0 +163.4T + 0.627 9T^2)×10^{-10}
Thermal conductivity of the TE materials ($W \cdot m^{-1} \cdot K^{-1}$)	$k_n=k_p$ =(62605.0 − 277.7T + 0.413T^2)×10^{-4}

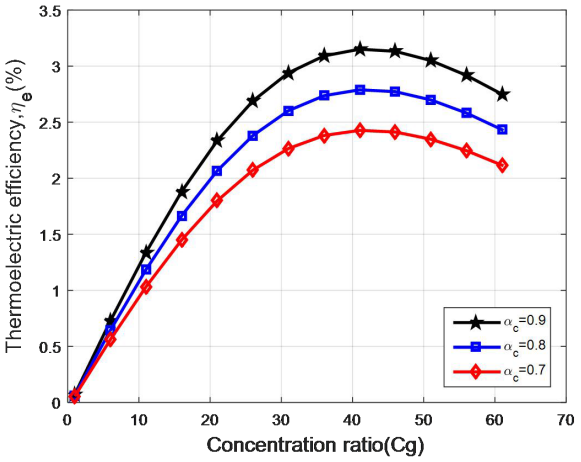

FIGURE 5. Influence of the absorption rate of the coating selective absorber on the conversion efficiency.

the TE module η_{TE} has a prominent effect on the conversion efficiency of the CTEG unit. However, η_{TE} depends on the temperature difference between the hot and cold ends of the TEG, which changes with the concentration ratio and the cooling condition of the phase change energy storage.

B. EFFECT OF THE FRESNEL SPOTLIGHT ON THE CTEG-PCM

The Fresnel lens is used to gather solar radiation on May 17th, 2019, in Beijing. The temperature curve of the hot end of the TEG before and after the concentration is shown in Fig. 6. In the figure, after using the Fresnel lens for focusing, the hot

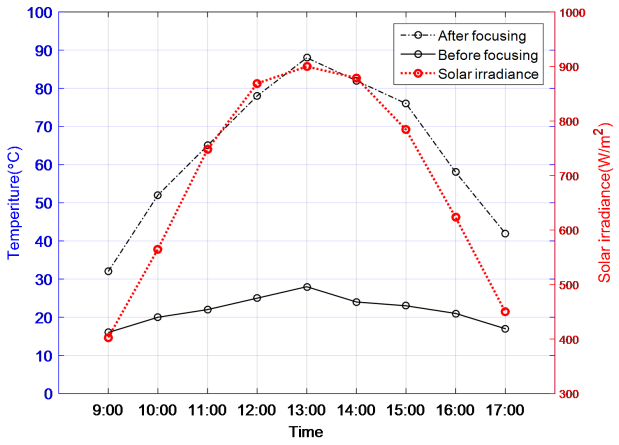

FIGURE 6. Temperature curve after focusing.

end temperature of the TEG is greatly improved, especially at 13 o'clock, where the hot end temperature of the TEG is the highest.

C. EFFECT OF THE PHASE CHANGE ENERGY STORAGE ON THE CTEG-PCM

It is known from Fig. 4a that the temperature at the hot end of the semiconductor thermometer reaches 353 K at a concentration ratio of 15. In the experiment, the 220 V and 100 W electric heater is selected to increase the temperature of the TEG hot end to a setting value of 353 K. When the heights of the exchanger are medium and short, the change curve of each measured value of the collected data is shown in Fig. 7.

In Fig. 7a, the height of the exchanger is in the medium. It shows that when the PCM melts near the melting point, the temperature changes little up or down. The aluminium fins of the heat exchanger effectively transfer thermal energy from the top of the container to the entire container. Therefore, temperature T_2 is stable at approximately 65°C within 10-30 minutes after the start of the experiment. When T_3 reaches 60°C, the heat source is turned off, but the hot end temperature T_1 has not reached the setting value at this time. In Fig. 7b, the height of the exchanger is in the short, showing that no matter how long the temperature T_1 has reached the setting value, T_3 is always around 56°C. Therefore, different heights of the exchanger have different PCM melting times to obtain different TEG electrical output performances. Furthermore, according to the maximum hot end temperature, the PCM parameters, such as the melting point and specific heat capacity, can be selected to obtain different TEG electrical output performances. Fig. 7 shows that even after the heat source is turned off, the PCM inside the container starts to release heat, which means that the entire unit will provide a longer temperature difference and generate a reverse voltage. The result shows that the CTEG-PCM unit can run in a full cycle; that is, it is used to generate electricity during the PCM melting and solidification process.

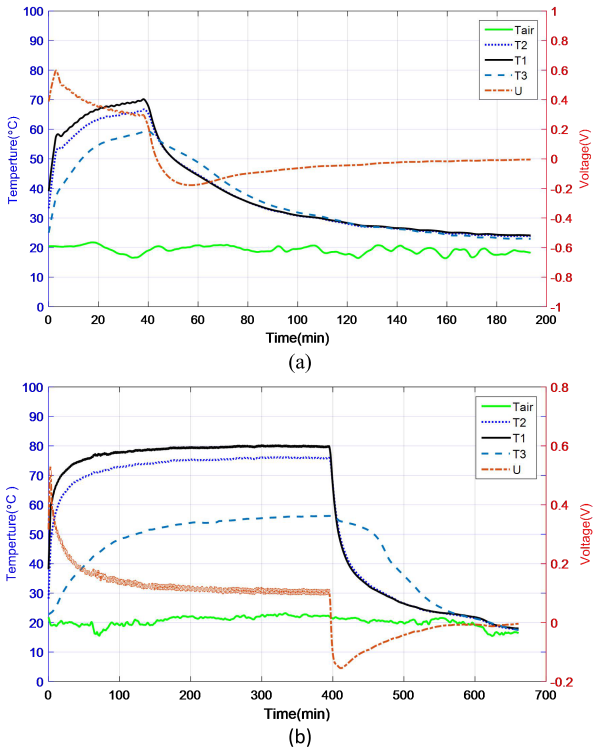

FIGURE 7. Time varying curve of the temperature and open circuit voltage: (a) the height of the exchanger is in the middle and (b) the height of the exchanger is short.

To better understand this phenomenon, the equivalent RC network can also be used to model the heat transfer in the PCM container, where R and C represent the thermal resistance and capacitance, respectively [34]. Since during the phase change, the PCM stores a large amount of energy at close-to-constant temperature, it acts similarly to a large thermal container and can be modelled as a capacitor. (16) and (17) define the thermal circuit elements, where h, w and l are the height, width and length of the elements, respectively. In addition, λ, ρ and C_{app} are the thermal conductivity, density and apparent heat capacity of the material, respectively.

$$R_{\text{th}} = \frac{h}{w \cdot l \cdot \lambda}, \tag{16}$$

$$C_{\text{th}} = l \cdot h \cdot w \cdot \rho \cdot C_{\text{app}}, \tag{17}$$

In (17), the apparent heat capacity of the material is kJ·kg^{-1}·K^{-1}. From (16), it can be observed that under a certain container size, the thermal conductivity of the material is an important part of the CTEG-PCM unit.

The same result is verified when the phase transition temperature of PCM is 35°C. The output open circuit voltage of the TEG is measured at the same setting temperature for different exchanger heights, as shown in Fig. 8.

In Figure 8, when the temperature at the bottom of the PCM container reaches the same value, the heater is removed directly and the voltage is dropped. It can be seen from the curve that when the height of the exchanger is the longest,

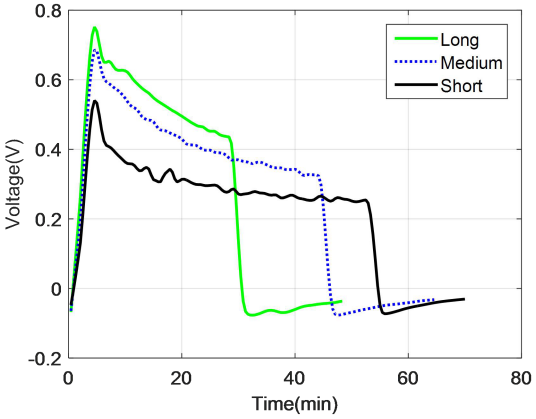

FIGURE 8. Open circuit voltage for different exchanger heights.

the medium and the shortest, then the duration for producing the forward open circuit voltage is 30 minutes, 44 minutes and 53 minutes, respectively, and the average forward voltage is 1.025 V, 0.4204 V and 0.299 V, respectively. Under three exchanger heights, the maximum reverse voltage values are basically equal to −0.079 V, but the time decrease to −0.04 V is 14 minutes, 12.5 minutes and 11 minutes. It can be seen that the thermal conductivity will affect the rate of energy absorption and the release of the CTEG-PCM unit. By improving the thermal conductivity, the thermal output can be increased, which directly affects the operation of the connected equipment. Since a micro-controller unit and a wireless sensor node can start up automatically with a 20 mV input voltage [1], the proposed CTEG-PCM unit is suitable for solving the self-power supply problem of the WSN nodes in forests. In fact, according to the boundary conditions and application, by optimizing the design of the exchanger, as well as the selection of the PCM, more voltage can be generated in a longer time, and the electrical performance of the system can be improved. The results of this experiment are consistent with those of reference [15].

VI. CONCLUSIONS

To analyse the application of a Fresnel lens and a PCM in a TEG system, the following conclusions are drawn:

1. The research results show that with an increase in the concentration ratio, the thermoelectric efficiency of the system increases, but the growth rate becomes slower. In practical applications, while seeking the highest conversion efficiency, attention should be paid to the maximum concentration ratio and the performance of the TE materials.

2. Increasing the absorption rate of the coating selective absorber can further improve the conversion efficiency of the system. When the conversion efficiency is the maximum, the absorption rate of the coating selective absorber is reduced by 0.1, and the conversion efficiency is reduced by 0.4%.

3. PCMs are beneficial for the thermal management of the cold end of the TEG. Phase change energy storage can reduce the fluctuation of the cold end temperature and increase

the power generation time. By optimizing the design of the exchanger, as well as the selection of the PCM, which can generate more voltage in a longer time, the electrical performance of the system can be improved.

The proposed CTEG-PCM unit is suitable for solving the self-power supply problem of WSN nodes in forests. The experimental tests were in the open circuit, further tests in a closed electrical circuit with an external load will be done.

REFERENCES

[1] M. Guan, K. Wang, D. Xu, and W.-H. Liao, "Design and experimental investigation of a low-voltage thermoelectric energy harvesting system for wireless sensor nodes," *Energy Convers. Manage.*, vol. 138, pp. 30–37, Apr. 2017.

[2] A. Dewan, S. U. Ay, M. N. Karim, and H. Beyenal, "Alternative power sources for remote sensors: A review," *J. Power Source*, vol. 245, pp. 129–143, Jan. 2014.

[3] J. W. Matiko, N. J. Grabham, S. P. Beeby, and M. J. Tudor, "Review of the application of energy harvesting in buildings," *Meas. Sci. Technol.*, vol. 25, no. 1, Jan. 2014, Art. no. 012002.

[4] W. Wang, V. Cionca, N. Wang, M. Hayes, B. O'Flynn, and C. O'Mathuna, "Thermoelectric energy harvesting for building energy management wireless sensor networks," *Int. J. Distrib. Sensor Netw.*, vol. 9, no. 6, Jun. 2013, Art. no. 232438.

[5] D. Milić, A. Prijić, L. Vračar, and Z. Prijić, "Characterization of commercial thermoelectric modules for application in energy harvesting wireless sensor nodes," *Appl. Thermal Eng.*, vol. 121, pp. 74–82, Jul. 2017.

[6] Z. Liu, B. Sun, Y. Zhong, X. Liu, J. Han, T. Shi, Z. Tang, and G. Liao, "Novel integration of carbon counter electrode based Perovskite solar cell with thermoelectric generator for efficient solar energy conversion," *Nano Energy*, vol. 38, pp. 457–466, Aug. 2017.

[7] M. Boonyasri, J. Jamradloedluk, C. Lertsatitthanakorn, A. Therdyothin, and S. Soponronnarit, "Increasing the efficiency of a thermoelectric generator using an evaporative cooling system," *J. Electron. Mater.*, vol. 46, no. 5, pp. 3043–3048, May 2017.

[8] X. Luo, Q. Guo, Z. Tao, Y. Liang, and Z. Liu, "Modified phase change materials used for thermal management of a novel solar thermoelectric generator," *Energy Convers. Manage.*, vol. 208, Mar. 2020, Art. no. 112459.

[9] M. E. Kiziroglou, T. Becker, S. W. Wright, E. M. Yeatman, J. W. Evans, and P. K. Wright, "Three-dimensional printed insulation for dynamic thermoelectric harvesters with encapsulated phase change materials," *IEEE Sensors Lett.*, vol. 1, no. 4, pp. 1–4, Aug. 2017.

[10] A. Agbossou, Q. Zhang, G. Sebald, and D. Guyomar, "Solar micro-energy harvesting based on thermoelectric and latent heat effects. Part I: Theoretical analysis," *Sens. Actuators A, Phys.*, vol. 163, no. 1, pp. 277–283, Sep. 2010.

[11] Q. Zhang, A. Agbossou, Z. Feng, and M. Cosnier, "Solar micro-energy harvesting based on thermoelectric and latent heat effects. Part II: Experimental analysis," *Sens. Actuators A, Phys.*, vol. 163, no. 1, pp. 284–290, Sep. 2010.

[12] M. Jaworski, M. Bednarczyk, and M. Czachor, "Experimental investigation of thermoelectric generator (TEG) with PCM module," *Appl. Thermal Eng.*, vol. 96, pp. 527–533, Mar. 2016.

[13] Y. Tu, W. Zhu, T. Lu, and Y. Deng, "A novel thermoelectric harvester based on high-performance phase change material for space application," *Appl. Energy*, vol. 206, pp. 1194–1202, Nov. 2017.

[14] S. A. Atouei, A. A. Ranjbar, and A. Rezania, "Experimental investigation of two-stage thermoelectric generator system integrated with phase change materials," *Appl. Energy*, vol. 208, pp. 332–343, Dec. 2017.

[15] S. A. Atouei, A. Rezania, A. A. Ranjbar, and L. A. Rosendahl, "Protection and thermal management of thermoelectric generator system using phase change materials: An experimental investigation," *Energy*, vol. 156, pp. 311–318, Aug. 2018.

[16] K. Karthick, S. Suresh, G. C. Joy, and R. Dhanuskodi, "Experimental investigation of solar reversible power generation in thermoelectric generator (TEG) using thermal energy storage," *Energy Sustain. Develop.*, vol. 48, pp. 107–114, Feb. 2019.

[17] M. E. Kiziroglou, S. W. Wright, T. T. Toh, P. D. Mitcheson, T. Becker, and E. M. Yeatman, "Design and fabrication of heat storage thermoelectric harvesting devices," *IEEE Trans. Ind. Electron.*, vol. 61, no. 1, pp. 302–309, Jan. 2014.

[18] D. Zhao and G. Tan, "Experimental evaluation of a prototype thermoelectric system integrated with PCM (phase change material) for space cooling," *Energy*, vol. 68, pp. 658–666, Apr. 2014.

[19] X. Zhou, C. Ma, L. Zhang, and P. Wang, "Design and performance experiment of solar concentrator with fixed strip mirror surface," *Trans. Chin. Soc. Agricult. Eng.*, vol. 30, no. 1, pp. 160–168, 2014.

[20] J. Wang, J. Wang, Y. Zhang, and X. Bi, "Analysis of heat transfer characteristics for parabolic trough solar collector," *Trans. Chin. Soc. Agricult. Eng.*, vol. 31, no. 7, pp. 185–192, 2015.

[21] K. Atik, "Numerical simulation of a solar thermoelectric generator," *Energy Sour., A, Recovery, Utilization, Environ. Effects*, vol. 33, no. 8, pp. 760–767, Feb. 2011.

[22] T. Cui, Y. Xuan, E. Yin, Q. Li, and D. Li, "Experimental investigation on potential of a concentrated photovoltaic-thermoelectric system with phase change materials," *Energy*, vol. 122, pp. 94–102, Mar. 2017.

[23] M. H. Nia, A. A. Nejad, A. M. Goudarzi, M. Valizadeh, and P. Samadian, "Cogeneration solar system using thermoelectric module and Fresnel lens," *Energy Convers. Manage.*, vol. 84, pp. 305–310, Aug. 2014.

[24] A. Kribus, "Thermal integral micro-generation systems for solar and conventional use," *J. Sol. Energy Eng.*, vol. 124, no. 2, pp. 189–197, May 2002.

[25] D. Z. Zhu and J. Liu, *Fundamentals of Solar Thermal Utilization*, vol. 4. Beijing, China: China Electric Power Press, 2017.

[26] M. Kalteh and H. A. Garmejani, "Investigating the influence of Thomson effect on the performance of a thermoelectric generator in a waste heat recovery system," *Int. J. Green Energy*, vol. 16, no. 12, pp. 917–929, Sep. 2019.

[27] B. V. K. Reddy, M. Barry, J. Li, and M. K. Chyu, "Mathematical modeling and numerical characterization of composite thermoelectric devices," *Int. J. Thermal Sci.*, vol. 67, pp. 53–63, May 2013.

[28] L. Cai, P. Li, Q. Luo, W. Huang, P. Zhai, and Q. Zhang, "Validation of discrete numerical model for thermoelectric generator used in a concentration solar system," *Proc. Inst. Mech. Eng., C, J. Mech. Eng. Sci.*, vol. 229, no. 3, pp. 465–475, Feb. 2015.

[29] Z.-G. Shen, S.-Y. Wu, L. Xiao, and G. Yin, "Theoretical modeling of thermoelectric generator with particular emphasis on the effect of side surface heat transfer," *Energy*, vol. 95, pp. 367–379, Jan. 2016.

[30] G. Fraisse, J. Ramousse, D. Sgorlon, and C. Goupil, "Comparison of different modeling approaches for thermoelectric elements," *Energy Convers. Manage.*, vol. 65, pp. 351–356, Jan. 2013.

[31] F. Agyenim, N. Hewitt, P. Eames, and M. Smyth, "A review of materials, heat transfer and phase change problem formulation for latent heat thermal energy storage systems (LHTESS)," *Renew. Sustain. Energy Rev.*, vol. 14, no. 2, pp. 615–628, Feb. 2010.

[32] E. Ogbonnaya, A. Gunasekaran, and L. Weiss, "Micro solar energy harvesting using thin film selective absorber coating and thermoelectric generators," *Microsyst. Technol.*, vol. 19, no. 7, pp. 995–1004, Jul. 2013.

[33] C.-C. Wang, C.-I. Hung, and W.-H. Chen, "Design of heat sink for improving the performance of thermoelectric generator using two-stage optimization," *Energy*, vol. 39, no. 1, pp. 236–245, Mar. 2012.

[34] A. Stupar, U. Drofenik, and J. W. Kolar, "Optimization of phase change material heat sinks for low duty cycle high peak load power supplies," *IEEE Trans. Compon., Packag., Manuf. Technol.*, vol. 2, no. 1, pp. 102–115, Jan. 2012.

XIAOMEI SUI was born in Benxi, Liaoning, China, in 1978. She received the B.S. and M.S. degrees in electronics engineering from Liaoning Shihua University, China, in 2003. She is currently pursuing the Ph.D. degree in forest engineering with Beijing Forestry University, China.

Since 2012, she has been an Associate Professor with the School of Electronic Information Engineering, North China Institute of Science and Technology. Her research interests include the development of thermal harvesting, modeling, simulations, and fabrication of a micro-structure systems.

WENBIN LI received the B.S. degree in forestry machine from Northeast Forestry University, Harbin, China, in 1982, the M.S. degree in forest engineering from Shizuoka University, Japan, in 1987, and the Ph.D. degree in forest engineering from Ehime University, Matsuyama, Japan, in 1990.

He is currently a Professor with Beijing Forestry University. His research interests include forest engineering and environment information monitoring.

YUQI ZHANG received the B.S. degree in mechanical engineering from Beijing Forestry University, China, in 2017, where she is currently pursuing the M.S. degree with the School of Technology. Her research mainly focuses on the micro-energy harvester and thermoelectric power generator combination, including research on the design of different structures and cooling systems of TEG.

YAFENG WU received the B.S. degree in mechanical design manufacturing and automation from Yantai University, China, in 2017. He is currently pursuing the M.S. degree with the School of Technology, Beijing Forestry University. His research focuses mainly on the heat transfer performance of a two-phase closed thermosiphon and the response characteristics of forest soil thermoelectric power generation systems.